

Big Entropy Fluctuations in the Nonequilibrium Steady State: A Simple Model with the Gauss Heat Bath[†]

B. V. Chirikov

Budker Institute of Nuclear Physics, Siberian Division, Russian Academy of Sciences, Novosibirsk, 630090 Russia
e-mail: *chirikov@inp.nsk.su*

Received July 6, 2000

Abstract—Large entropy fluctuations in a nonequilibrium steady state of classical mechanics are studied in extensive numerical experiments on a simple two-freedom model with the so-called Gauss time-reversible thermostat. The local fluctuations (on a set of fixed trajectory segments) from the average heat entropy absorbed in the thermostat are found to be non-Gaussian. The fluctuations can be approximately described by a two-Gaussian distribution with a crossover independent of the segment length and the number of trajectories (“particles”). The distribution itself does depend on both, approaching the single standard Gaussian distribution as any of those parameters increases. The global time-dependent fluctuations are qualitatively different in that they have a strict upper bound much less than the average entropy production. Thus, unlike the equilibrium steady state, the recovery of the initial low entropy becomes impossible after a sufficiently long time, even in the largest fluctuations. However, preliminary numerical experiments and the theoretical estimates in the special case of the critical dynamics with superdiffusion suggest the existence of infinitely many Poincaré recurrences to the initial state and beyond. This is a new interesting phenomenon to be further studied together with some other open questions. The relation of this particular example of a nonequilibrium steady state to the long-standing persistent controversy over statistical “irreversibility”, or the notorious “time arrow”, is also discussed. In conclusion, the unsolved problem of the origin of the causality “principle” is considered. © 2001 MAIK “Nauka/Interperiodica”.

1. INTRODUCTION: EQUILIBRIUM VS. NONEQUILIBRIUM STEADY STATE

Fluctuations are an inseparable part of statistical laws. This has been well known since Boltzmann. What is apparently less known are the peculiar properties of rare big fluctuations (BF) as different from, and in a sense even opposite to, those of small stationary fluctuations. In particular, the former can be perfectly regular on the average, symmetric in time with respect to the fluctuation maximum, and can be described by simple kinetic equations rather than by a sheer probability of irregular “noise”. Even though big fluctuations are very rare, they may be important in many various applications (see, e.g., [1] and references therein). In addition, the correct understanding and interpretation of the properties and origin of big fluctuations may help (at last!) to settle a strangely persistent controversy over statistical “irreversibility” and the notorious “time arrow”.

In the big fluctuations problem, one must distinguish at least two qualitatively different classes of the fundamental (Hamiltonian, nondissipative) dynamical systems: those with and without the statistical equilibrium, or the equilibrium steady state (ES).

In the former (simpler) case, a big fluctuation consists of the two symmetric parts: the rise of a fluctuation

followed by its return, or relaxation, back to ES (see Fig. 1 below). Both parts are described by the same kinetic (e.g., diffusion) equation, the only difference being in the sign of time. This relates the time-symmetric dynamical equations to the time-antisymmetric kinetic (but not statistical!) equations. The principal difference between the two, sometimes overlooked, is that the kinetic equations are widely understood as describing the relaxation only, i.e., the increase of the entropy in a closed system, whereas they actually do so for the rise of the big fluctuation as well, i.e., for the entropy decrease. All this was qualitatively known already to Boltzmann [2]. The first simple example of a symmetric big fluctuations was considered by Schrödinger [3]. A rigorous mathematical theorem for the diffusion (slow) kinetics was proved by Kolmogorov in 1937 in the paper entitled “Zur Umkehrbarkeit der statistischen Naturgesetze” (“Concerning the Reversibility of Statistical Laws in Nature”) [4] (see also [5]). Regrettably, the principal Kolmogorov theorem still remains unknown to participants of the heated debate over “irreversibility” (see, e.g., “Round Table on Irreversibility” in [6]) and to the physicists actually studying such big fluctuations [1].

By now, there exists the well developed ergodic theory of dynamical systems (see, e.g., [7]). In particular, it proves that the relaxation (correlation decay, or mixing) proceeds eventually in both directions of time for almost any initial conditions of a chaotic dynamical

[†]This article was submitted by the author in English.

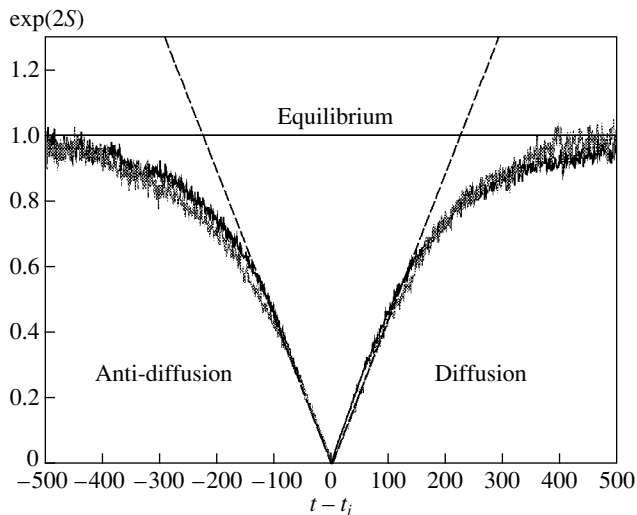


Fig. 1. Boltzmann's diffusive fluctuations in model (1.2) with the parameter $C = 15$: the square of the phase space area occupied by N independent trajectories ("particles") vs. the time (the number of map iterations $t - t_i$) counted from the instant t_i of fluctuation maximum, or of minimal Γ_{fl} , for each of the N_{fl} superimposed big fluctuations separated by the average period $P = \langle (t_i - t_{i-1}) \rangle$. Straight lines show the expected dependence for anti-diffusion and diffusion (see text). Two slightly different curves correspond to $N = 1$ (grey) and $N = 4$ (black) with $\Gamma_{fl} = 0.0001$ and 0.1 : $N_{fl} = 3352$ and 2851 ; $P = 29863$ and 35110 , respectively.

system. However, the relaxation must not always be monotonic, which simply means a big fluctuation on the way, depending on the initial conditions. To eliminate this apparently confusing (to many) "freedom," one can take a different approach to the problem: to start at arbitrary initial conditions (most likely corresponding to ES) and see the big fluctuation dynamics and statistics.

At this point, it is essential to recall that the systems with ES allow for very simple models in both the theoretical analysis and numerical experiments (of which the latter are even more important). In this paper, we use one of the most simple and popular models specified by the so-called Arnold cat map (see [8, 9])

$$\begin{aligned} \bar{p} &= p + x \pmod{1}, \\ \bar{x} &= x + \bar{p} \pmod{1}, \end{aligned} \quad (1.1)$$

that is a linear canonical map on the unit torus. It has no parameters and is chaotic and even ergodic. The rate of the local exponential instability, the Lyapunov exponent

$$\lambda = \ln(3/2 + \sqrt{5}/2) = 0.96,$$

implies a fast (ballistic) kinetics with the relaxation time $t_r \sim 1/\lambda \approx 1$.

A minor modification of this map,

$$\bar{p} = p + x - \frac{1}{2} \pmod{C}, \quad (1.2)$$

$$\bar{x} = x + \bar{p} \pmod{1},$$

where $C \gg 1$ is the circumference of the phase space torus admits a slow (diffusive) relaxation with

$$t_r \sim C^2/4D_p,$$

where $D_p = 1/12$ is the diffusion rate in p . A convenient characteristic of the big fluctuation size is the rms phase space volume (area) $\Gamma(t) = \sigma_p \sigma_x$ for a group of N trajectories. In the ergodic motion at equilibrium, we have

$$\Gamma = \Gamma_0 = C/12.$$

In what follows, we use the dimensionless measure

$$\tilde{\Gamma} = \Gamma/\Gamma_0 \longrightarrow \Gamma$$

and omit the tilde.

The entropy S can be defined by the relation

$$S(t) = \ln \Gamma(t), \quad (1.3)$$

with $S = 0$ at equilibrium. This definition is not identical to the standard one (via the (coarse-grained) distribution function) but it is quite close to the latter if $\Gamma \ll 1$, i.e., for a big fluctuation, which is what we need in the problem under consideration. A great advantage of definition (1.3) is that the computation of S does not require very many trajectories as does the distribution function. In fact, even a single trajectory is sufficient!

A finite number of trajectories used for calculating the phase-space volume Γ is a sort of the coarse-grained distribution, as required in relation (1.3), but with a free bin size that can be arbitrarily small. The detailed study of big fluctuations in this class of ES models will be published elsewhere [10]. Here, we briefly consider the example shown in Fig. 1.

The data were obtained from running 4 and only 1 (!) trajectories for a sufficiently long time in order to collect sufficiently many big fluctuations; they are superimposed in Fig. 1 to clean up the regular big fluctuation from a "podlike trash" of stationary fluctuations. The size of big fluctuation chosen was approximately fixed by the condition $\Gamma(t) \leq \Gamma_{fl}$. In spite of the inequality, the mean values $\langle \Gamma(t_i) \rangle = 0.000033$ and 0.069 are close (by the order of magnitude) to the fixed Γ_{fl} values in Fig. 1. We note that for a slow diffusive kinetics, we have

$$\exp(2S) \propto \sigma_p^2 \propto \langle p^2 \rangle$$

and σ_x remains constant.

The probability of big fluctuations can be characterized by the average period between them, for which a very simple estimate

$$P \approx 3\Gamma_{fl}^{-N} \approx 3\exp(-NS_{fl}) \quad (1.4)$$

is in a good agreement with data in Fig. 1 (upon including the empirical factor 3).

In the example presented here, the position of all big fluctuations in the phase space is fixed as $x_{fl} = 1/2$ and $p_{fl} = C/2$. If one lifts this restriction, the probability of big fluctuation increases by the factor $1/\Gamma_{fl}$, or by decreasing N by one ($N \rightarrow N - 1$), due to the arbitrary position of a big fluctuation in phase space. In the former case, a chain of big fluctuations is precisely the well known Poincaré recurrence. It is less known that the latter are a particular and specific case of big fluctuations, and the recurrence of a trajectory in a chaotic system is determined by the kinetics of the system. The recurrence of several ($N > 1$) trajectories can also be interpreted as the recurrence of a single trajectory in N uncoupled freedoms.

As can be seen from Fig. 1, irregular deviations from a regular big fluctuation are rapidly decreasing with the entropy $S \rightarrow S_{fl}$. It may seem that the motion becomes regular near big fluctuation maximum, hence the term “optimal fluctuational path” [1]. In fact, the motion remains diffusive down to the dynamical scale, that is, $|\Delta p| \sim 1$ independently of parameter C in model (1.2).

Big fluctuations are not only perfectly regular by themselves but also surprisingly stable against any perturbations, both regular and chaotic. Moreover, the perturbations do not need to be small. At first glance, this looks very strange in a chaotic, highly unstable dynamics. The resolution of this apparent paradox is that the dynamical instability of motion affects the big fluctuation time instant t_i only. The big fluctuation shape is determined by the kinetics that can have an arbitrary mechanism, ranging from a purely dynamical one, as in model (1.2), to a completely noisy (stochastic, cf. Fig. 1 above and Fig. 4 in [1]). As a matter of fact, the fundamental Kolmogorov theorem [4] is specifically related to the latter case but remains valid in a much more general situation. The surprising stability of big fluctuations is similar to the full (less known) robustness property of the Anosov (strongly chaotic) systems [11], whose trajectories are only slightly deformed under a small perturbation (for discussion, see [12]). From a different perspective, this stability can be interpreted as a fundamental property of the “macroscopic” description of big fluctuations. In such a simple few-freedom system similar to (1.2), the term “macroscopic” refers to the averaged quantities σ , Γ , S , and similar ones. However, a somewhat confusing result is that the “macroscopic” stability comprises not only the relaxation of big fluctuations but also its rise, because both parts of big fluctuation always appear together. This may lead to another misunderstanding that the fluctuation and relaxation probabilities are the same, which is certainly wrong. The point is that the ratio of

both (unequal!) probabilities is determined by the crossover parameter

$$R_{cro}(S_{fl}) = \frac{P}{t_r} \approx \frac{3 \exp(-NS_{fl})}{C^2} \gg 1, \quad (1.5)$$

where the latter expression refers to model (1.2) and the inequality determines the region of a big fluctuation where its waiting time is much longer than that of its immediate relaxation from a nonequilibrium “macroscopic” state (for further discussion, see Section 6 in what follows).

2. A NEW CLASS OF DYNAMICAL MODELS: WHAT ARE THEY FOR?

A relatively simple picture of big fluctuations in systems with the equilibrium steady state is well understood by now, although not yet well known. To Boltzmann, this picture was the basis of his fluctuation hypothesis for our Universe. Again, as is well understood by now, this hypothesis is entirely incompatible with the present structure of the Universe, because it would immediately imply the notorious “heat death” (see, e.g., [13]). For this reason, one may even term such systems the heat death models. Nevertheless, they can be and actually are widely used in the description and study of local statistical processes in thermodynamically closed systems. The latter term means the absence of any heat exchange with the environment. We note, however, that for exponentially unstable motion, the only dynamically closed system is the whole Universe. In particular, this excludes the hypothetical “velocity reversal,” which is still popular in debates over “irreversibility” occurring since Loschmidt (for discussion, see, e.g., [12, 14] and Section 6 in what follows).

In any event, dynamical models with ES do not tell us the whole story of either the Universe or even a typical macroscopic process therein. The principal solution of this problem, unknown to Boltzmann, is quite clear by now, namely, the “equilibrium-free” models are wanted. Various classes of such models are intensively studied today. Moreover, the celebrated cosmic microwave background tells us that our Universe was born already in the state of a heat death; fortunately to us, however, it became unstable because of the well-known Jeans gravitational instability [15]. This resulted in developing a rich variety of collective processes, or synergetics, the term recently introduced or, better to say, put in use by Haken [16]. The most important peculiarity of this collective instability is in that the total overall relaxation (to somewhere?) with ever increasing total entropy is accompanied by an also increasing phase space inhomogeneity of the system, particularly in temperature. In other words, the whole system as well as its local parts become more and more nonequilibrium to the extent of the birth of a secondary dynamics that can be, and sometimes is, as perfect as,

for example, the celestial mechanics (for general discussion see, e.g., [17, 18, 12]).

We stress that all these inhomogeneous nonequilibrium structures are not big fluctuations as in ES systems, but are a result of regular collective instability, and therefore, they are immediately formed under a certain condition. In addition, they are typically dissipative structures in Prigogine's terms [19] because of the energy and entropy exchange with the infinite environment. The latter is the most important feature of such processes, and at the same time the main difficulty in studying the dynamics of those models both theoretically and in numerical experiments, which are so much simpler for the ES systems. Usually, the investigations in this field are based upon statistical laws omitting the underlying dynamics from the beginning.

Recently, however, a new class of dynamical models has been developed by Evans, Hoover, Morriss, Nosé, and others [20, 21]. Some researchers still hope that these new models will help to resolve the "paradox of irreversibility." A more serious reason for studying these models is that they allow one to relatively simply include the infinitely dimensional "thermostat," or "heat bath" into a model with a few degrees of freedom. This greatly facilitates both numerical experiments and the theoretical analysis. In particular, a derivation of the Ohm law within this model was presented in [22], thereby solving "one of the outstanding problems of modern physics" [23] (for this peculiar dynamical model only!). The authors of [22] claim that "At present, no general statistical mechanical theory can predict which microscopic dynamics will yield such transport laws...." In my opinion, it would be more correct to inquire which of many relevant models could be treated theoretically, and especially in a rigorous way as was actually done in [22].

The zest of new models is the so-called Gauss thermostat, or heat bath (GHB). In the simplest case, the motion equations of a particle in this bath are [20–22]:

$$\frac{d\mathbf{p}}{dt} = \mathbf{F} - \zeta\mathbf{p}, \quad \zeta = \frac{\mathbf{F} \cdot \mathbf{p}}{p^2}, \quad (2.1)$$

where \mathbf{F} is a given external force and ζ stands for the "friction coefficient." The first peculiarity of this "friction" is in its explicit time reversibility contrary to the "standard friction." The price for reversibility is the strict connection between the two forces, the friction and the external force \mathbf{F} . Moreover, and this is most important, the connection is such that

$$|\mathbf{p}|^2 = p_0^2 = \text{const}$$

is the exact motion invariant,

$$\frac{d|\mathbf{p}|^2}{dt} = \mathbf{p} \cdot \frac{d\mathbf{p}}{dt} = \mathbf{p} \cdot \mathbf{F} - \mathbf{F} \cdot \mathbf{p}. \quad (2.2)$$

The first of the two identical terms represents the mechanical work of the external regular force \mathbf{F} , the

spring of the external energy, and the second one describes the sink of energy into GHB. Thus, asymptotically as $t \rightarrow \infty$, the model describes a steady state only. This is the main restriction of such models. The particle itself does only immediately transfer the energy without any change of its own because of the above constraint

$$|\mathbf{p}|^2 = \text{const}.$$

For a single degree of freedom, the latter would lead to the trivial solution $p = \text{const}$. Therefore, at least two degrees of freedom are required to allow for a variation of vector \mathbf{p} in spite of the constraint. For many interacting particles, the constraint

$$\sum |\mathbf{p}_i|^2 = \text{const}$$

is less stringent, hence the reference to the Gauss "Principle of Least Constraint" [24] for deriving the reversible friction in Eq. (2.1). In the present paper, the simplest case of N noninteracting particles with two degrees of freedom is considered only as in [22].

The next important point is a special form of the energy in GHB, which is the heat. In true heat bath it is given by the chaotic motion of infinitely many particles. This is not the case in GHB, and one needs an additional force in Eq. (2.1) to make the particle motion chaotic, at the same time maintaining the constraint. Whether such an external to GHB chaos is equivalent to the chaos inside the true heat bath, at least statistically, remains an open question, but it seems plausible from the physical viewpoint [22] (see also [25]). If so, the model describes the direct conversion of mechanical work into heat Q , and hence the permanent entropy production. The calculation of the latter is not a trivial question (for discussion, see [20–22]). In our opinion, the simplest way is to use the thermodynamic relation

$$\frac{dS}{dt} = \frac{1}{T} \frac{dQ}{dt}, \quad \frac{dQ}{dt} = \mathbf{p} \cdot \mathbf{F}, \quad (2.3)$$

where $T = p_0^2$ is the effective temperature [22]. Because the input energy is of zero entropy (the formal temperature $T_{in} = \infty$), relation (2.3) determines the entropy production in the whole system (particles + GHB). We note that in Eq. (2.3), as well as throughout this paper, the entropy S is understood to be determined in the standard way via a coarse-grained distribution function.

On the other hand, the usual interpretation of GHB models is quite different [20–22]. Namely, the entropy production in Eq. (2.3) is expressed via the Lyapunov exponents λ_i of the particle motion,

$$\frac{dS}{dt} \equiv \frac{dS_{GHB}}{dt} \equiv -\frac{dS_p}{dt} = -\sum_i \lambda_i, \quad (2.4)$$

where S_{GHB} and S_p are the respective entropy of GHB and of the ensemble of particles. An unpleasant feature

of this relation is in that the latter equality holds for the Gibbs entropy only, which is conserved in the Hamiltonian system modeled by the GHB. As a result, the entropy of the total system (particle + GHB) remains constant (the second equality in Eq. (2.4)), which literally means no entropy production at all! Even though this interpretation can be formally justified, it seems to us to be physically misleading. In our opinion, the application of Lyapunov exponents would be better restricted to characterization of the phase-space fractal microstructure of the particle motion (which is really interesting), retaining the universal coarse-grained definition of the entropy (cf. ES models in Section 1).

As mentioned above, the GHB models describe the nonequilibrium steady states only. Moreover, any collective processes of interacting particles are also excluded, among them those responsible for the very existence of regular nonequilibrium processes, in particular, of field \mathbf{F} in model (2.1). In a more complicated Nosé–Hoover version of GHB models, these severe restrictions can be partly, but not completely, lifted. Whether this is sufficient for the inclusion of collective processes remains, to my knowledge, an open question.

In any event, even the simplest GHB model like (2.1) represents a qualitatively different type of statistical behavior compared to that in the ES models. The origin of this principal difference is twofold: (i) the external “inexhaustible” spring of energy, if only introduced “by hand”, and (ii) a heat sink of infinite capacity that excludes any equilibrium.

In conclusion of this section, we precisely formulate the model considered in the main part of the paper. Choosing the model for numerical experiments, I follow my favored the “golden rule”: construct the model as simple as possible but not simpler. In the problem under consideration, the models already studied are mainly based on the well-known and well-studied “Lorentz gas” that is a particle (or many particles) moving through a set of fixed scatterers. A new element is a constant field accelerating the particles. Actually, the Lorentz model becomes the famous Galton Board [26], the very first model of chaotic motion, which was invented by Galton for another purpose, and which has not been studied in detail until recently [20–22]. Our model is still simpler, and is specified by the two maps: (i) the 2D Arnold cat map (1.1) to chaoticize particles, and (ii) the 1D map version of Eq. (2.1),

$$\overline{p}_1 = p_1 + F - 4Fp_1^2, \quad (2.5)$$

where $p_1 = p - p_0$ and the parameter in Eq. (2.1) is $p_0 = 1/2$. For $|F| < 1/4$, the momentum p remains within the unit interval ($0 \leq p \leq 1$) as in map (1.1). The principal relation (2.3) for the entropy reduces also to the additional 1D map,

$$\bar{S} = S + (p_1 + F)^2 - p_1^2 = S + 2p_1F + F^2, \quad (2.6)$$

where the entropy unit is changed by the factor 2 for simplicity. Because S is the entropy produced in GHB,

the latter map implicitly includes also the motion in the second degree of freedom for each of the noninteracting particles because of the Gauss constraint that guarantees the immediate transfer of energy to GHB.

In numerical experiments considered below, an arbitrary number N of noninteracting particles (trajectories) with random initial conditions was used. In this case, the Gauss constraint remains unchanged, and all the trajectories are run simultaneously.

3. NONMONOTONIC ENTROPY PRODUCTION: LOCAL FLUCTUATIONS

The statistical properties of entropy growth in the model chosen are determined by the first two moments of the p_1 distribution function. In the limit as $t \rightarrow \infty$ and/or $N \rightarrow \infty$, they are given by (per iteration and per trajectory)

$$\langle p_1 \rangle = 0, \quad \langle p_1^2 \rangle = \frac{1}{12}, \quad (3.1)$$

where averaging is done over both the motion time t (now the number of the iterations of the map) and N noninteracting particles (particle trajectories). In combination with Eq. (2.6), the first moment in Eq. (3.1) implies the linear growth of the average entropy (per trajectory),

$$\langle S(t) \rangle = tF^2. \quad (3.2)$$

In this section, the statistics of local fluctuations is considered. A similar problem was studied in [27] for a more realistic model with many interacting particles. In the present model, the local fluctuation is defined as follows. The total motion time t_f is subdivided into many segments of equal duration t_1 . On each segment $i = 1, \dots, t_f/t_1$, the total change of the entropy S_i for all N trajectories is calculated using Eq. (2.6) and represented as the dimensionless random variable

$$S_\sigma = \frac{S_i - \langle S_i \rangle}{\sigma} = \frac{S_i - \tau}{\sigma}, \quad (3.3)$$

where

$$\langle S_i \rangle = Nt_1F^2 = \tau$$

(see Eq. (3.2)), and the rms fluctuation σ is given by a simple relation (see Eqs. (2.6) and (3.1))

$$\sigma^2 = \frac{\tau}{3}. \quad (3.4)$$

This relation neglects all the correlations, which implies the standard Gaussian distribution

$$G(S_\sigma) = \frac{\exp(-S_\sigma^2/2)}{\sqrt{2\pi}}. \quad (3.5)$$

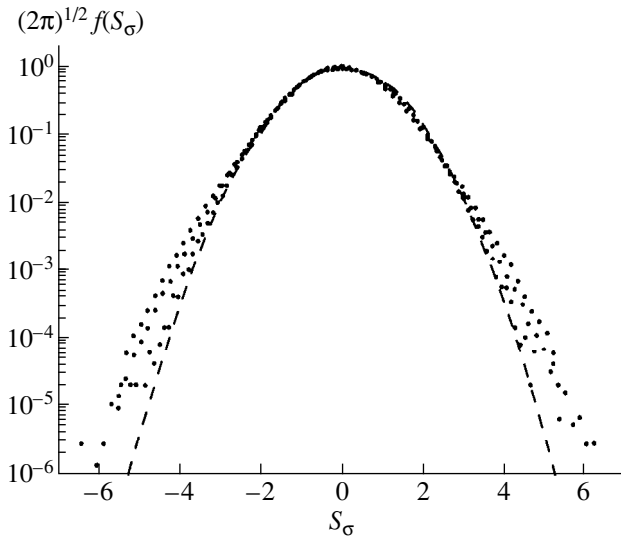


Fig. 2. Distribution function $f(S_G)$ of local fluctuations in the nonequilibrium steady state with $F = 0.01$. Dashed line is the standard Gauss law (3.5); points represent the results of numerical experiments with $N = 1$ and $t_1 = 10, 25, 100$.

An example of the actual distribution function is shown in Fig. 2 for a single trajectory with the segment length $t_1 = 10, 25, 100$ iterations, and the number of segments up to 10^7 . The cap of the distribution is close to the standard Gauss form (3.5) (see also Fig. 3) but both tails clearly show a considerable enhancement of fluctuations depending on both t_1 and N (in other examples, see below).

The shape of the tails is also Gaussian but the width is larger the smaller t_1 and N . This is especially clear in a different representation of the data in Fig. 3, where the ratio of the empirical distribution to the standard Gauss one is plotted as a function of the Gaussian variable $S_G = S_G^2/2$. Each run with particular values of N and t_1 is represented by two slightly different lines for both signs of S_G . In addition to fluctuations, the difference apparently involves some asymmetry of the distribution with respect to $S_G = 0$. The origin of this asymmetry is not completely clear as yet. A sharp crossover between the two Gaussian distributions at $S_G \approx 3$ is nearly independent of the parameters N and t_1 , as is the top distribution below crossover. On the contrary, the tail distribution essentially depends on both parameters in a rather complicated way. The origin of the difference between the two Gaussian distributions apparently lies in dynamical correlations. In spite of a fast decay (see Section 1), the correlation in Arnold map (1.1) does affect somehow the big entropy fluctuations except in the limiting case $N \gg t_1$ (two lower lines in Fig. 3), where the correlations vanish because of random and statistically independent initial conditions of many trajectories.

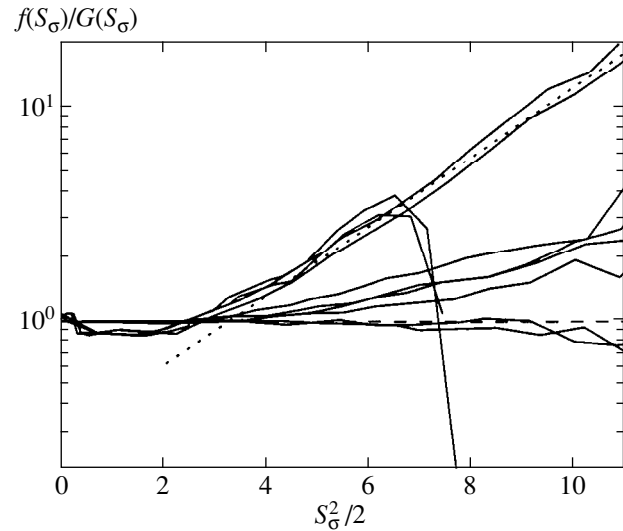


Fig. 3. The ratio of the distribution $f(S_G)$ to the standard Gauss law (3.5) (broken lines). The values of the parameter N/t_1 from top to bottom are: $1/5$ ($S_G^2/2 < 7.5$, see text); $1/10$; $1/100$; $10/10$, and $100/1$. The oblique dotted straight line demonstrates the Gaussian shape of the tails.

For any fixed parameters N and t_1 , the fluctuations are bounded ($F \ll 1$),

$$|S_G| < \sqrt{3Nt_1}, \quad (3.6)$$

which follows from Eqs. (2.6), (3.3), and (3.4). This is clearly seen in Fig. 3 for minimal $Nt_1 = 5$. If only force F is fixed instead, the relative entropy fluctuations

$$\frac{S_i}{\langle S_i \rangle} \approx \pm \frac{1}{F} \quad (3.7)$$

are also restricted but can be arbitrarily large for small F and, moreover, can have either sign. This implies a nonmonotonic growth of the entropy at the expense of the segments with $S_i < 0$.

The probability (in the number of trajectory segments) of extremely large fluctuations, Eqs. (3.6) and (3.7), is exponentially small (see Eq. (3.5) and below). However, the probability of the fluctuations with a negative entropy change ($S_i < 0$) (without time reversal!) is generally not small at all, reaching 50% as $\tau \rightarrow 0$ (for arbitrary N and t_1). In principle, this is known, at least for the systems with an equilibrium steady state (Section 1). Nevertheless, the first, to my knowledge, direct observation of this phenomenon in a nonequilibrium steady state [27] has so much staggered the authors that they even entitled the paper ‘‘Probability of Second Law violations in Shearing Steady State’’. In fact, this is simply a sort of peculiar fluctuations that are big not so much with respect to their size but primarily to their probability (cf. discussion in Section 1). However, the important point is that all those negative entropy fluctuations (transforming the heat into work) are randomly

scattered among the others of positive entropy, and for making any use of the former a Maxwell's demon is required who is known by now to be well in a "peaceful coexistence" with the Second Law.

A Gaussian distribution of the entropy fluctuations shifted with respect to $S_i = 0$ in a nonequilibrium steady state first observed in [27] was also theoretically explained there in terms of the Lyapunov exponents (see Eq. (8) in [27]). This was the first form of what is now called the "Fluctuation Theorem" (see, e.g., D. Ruelle in [6, p. 540]). In my opinion, a more physical representation of this theorem would be the ratio of the two moments in Eq. (3.4). In any representation, the theorem essentially depends on both the underlying dynamics and the type of fluctuations considered (see Sections 4 and 5).

Another interesting limit is $t_1 \rightarrow t_f \rightarrow \infty$ (a single segment) [27] with $\tau \rightarrow 0$, which is possible if $F \rightarrow 0$ too. In this case, the probability of zero entropy change in the entire motion also approaches 50%. However, the probability of any negative entropy fluctuation vanishes (see Eq. (3.3)). An interesting question is whether there exists some intermediate region of parameters where the latter probability remains finite. In other words, are the Poincaré recurrences to negative entropy change $S_i < 0$ possible in a nonequilibrium steady state as these are in the equilibrium (Section 1)? The answer to this question is given by the statistics of the global fluctuations.

4. NONMONOTONIC ENTROPY PRODUCTION: GLOBAL FLUCTUATIONS

The definition of the global fluctuations is similar to, yet essentially different from that of the local fluctuations in the previous section. Namely (cf. Eqs. (3.3) and (3.4)), the principal dimensionless random variable $S_\sigma(t)$ now explicitly depends on time,

$$S_\sigma(t) = \frac{S(t) - \langle S(t) \rangle}{\sigma} = \frac{S(t) - \tau}{\sigma}, \quad (4.1)$$

where $S(t)$ is calculated from Eq. (2.6), $S(0) = 0$, $\langle S(t) \rangle = NtF^2 \equiv \tau$ (see Eq. (3.2)), and the rms fluctuation σ is given by the same relation (3.4) with a new time variable τ ,

$$\sigma^2 = \frac{\tau}{3}. \quad (4.2)$$

In other words, the global fluctuations are described as a diffusion with the constant rate

$$D = \frac{\sigma^2}{\tau} = \frac{1}{3}. \quad (4.3)$$

The global fluctuations can also be viewed as a continuous time-dependent deviation of the entropy from its average growth unlike the local fluctuations in the ensemble of fixed trajectory segments (Section 3).

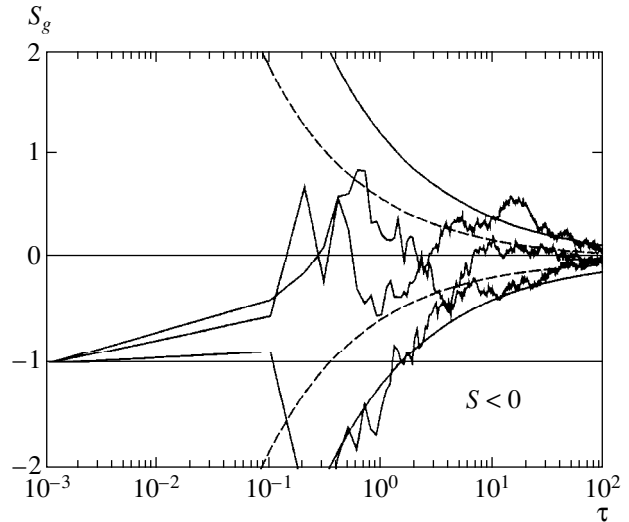


Fig. 4. Time dependence of the reduced global fluctuations $S_g(\tau)$, Eq. (4.4): three sets by $N = 10$ trajectories with different initial conditions but the same initial entropy $S(0) = 0$ and $F = 0.01$. Horizontal solid line $S_g = 0$ represents the average entropy growth. The lower solid line $S = 0$ is the border between positive and negative entropy growth. A pair of dashed curves corresponds to the standard rms fluctuation σ , Eq. (4.2), and two solid curves represent the maximum diffusion fluctuations σ_b , Eq. (4.5).

Now, the primary goal is to find whether the entropy can reach negative values $S(t) < 0$ as $t \rightarrow \infty$. As was discussed in the previous section, this is possible at some finite segments of the trajectory with the probability rapidly decreasing (but always finite) as the segment length grows.

In Fig. 4, three examples of global fluctuations are shown in a slightly different representation (cf. Eq. (4.1))

$$S_g(\tau) = \frac{S(\tau)}{\tau} - 1 \quad (4.4)$$

chosen in order to always keep the most important border $S(\tau) = 0$ in front of one's eyes (with $S_g(\tau) = -1$, the horizontal line in Fig. 4). Eventually, all trajectories converge to the average entropy growth (the horizontal line $S_g = 0$ in Fig. 4). During the initial stage of diffusion, the probability of negative entropy is roughly 50%, similar to the local fluctuations (Section 3). However, the situation cardinally changes at $t \approx 1$, with all the trajectories moving away from the border $S = 0$. Moreover, the relative distance to the border with respect to the fluctuation size increases indefinitely.

The fluctuation size is characterized by two parameters. The first one is the well-known rms dispersion σ , Eq. (4.2) (two dashed curves in Fig 4), which estimates the fluctuation distribution width. In the problem under consideration, the most important is the second characteristic, σ_b (two solid curves in Fig. 4), which sets the maximum size (the upper bound) of the diffusion fluctuations, and therefore insures against the recurrence

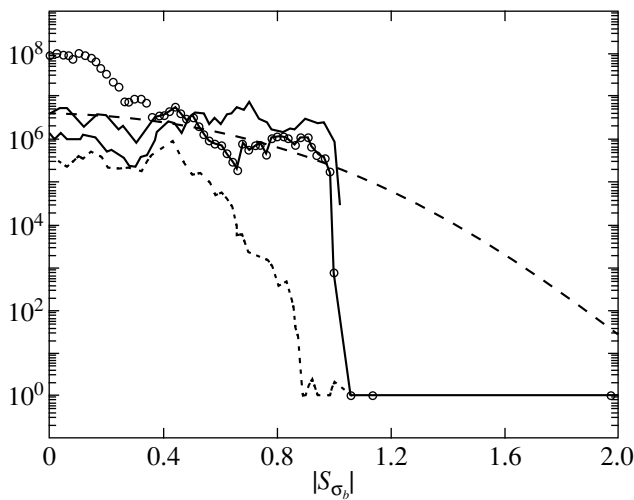


Fig. 5. Histogram of the global fluctuations in the number of entries per bin of the width 0.02: $F = 0.01$; $N = 100$; $R_\sigma \approx 3$. From bottom to top in the left-most part of figure: $\tau = 10^5$ (dashed line); 10^6 (two solid lines, different initial conditions); 10^7 (circles); the total motion time $t = 100\tau$ iterations. For comparison, the smooth dashed line shows unbounded Gaussian distribution (4.7) for $\tau = 10^6$.

into the region $S < 0$ in a sufficiently long time. The ratio of the two sizes

$$R_\sigma(\tau) = \frac{\sigma_b}{\sigma} = \sqrt{2 \ln \ln(A\tau)} \quad (4.5)$$

is given by the famous Khinchin law of iterated logarithms [28].

We emphasize again that the principal peculiarity and importance of the border σ_b is that it characterizes a sharp drop of the fluctuation probability down to zero (in the limit as $\tau \rightarrow \infty$). In other words, almost any trajectory approaches infinitely many times arbitrarily close to this border from below, but the number of border crossings remains finite. In Fig. 4, this corresponds to the eternal confinement of trajectories in the gap between the two solid curves.

This surprising behavior of random trajectories is well known to mathematicians but, apparently, not to physicists. In Fig. 5 several examples of the fluctuation distributions are shown for illustration of that impenetrable border.

In the Khinchin theorem, factor A in Eq. (4.5) is irrelevant and is set to $A = 1$. This is because the theorem can be proved in the formal limit as $\tau \rightarrow \infty$, only as most theorems in the probability theory (as well as in the ergodic theory, by the way). However, in numerical experiments on a finite time, even if arbitrarily large, one needs a correction to the limit expression. In addition, it would be desirable to look at the border over the whole motion down to the dynamical time scale determined by the correlation decay. In the model under consideration, it is of the order of the relaxation time $t_r \sim 1$

(see Section 1). The additional parameter A can be fixed by the condition

$$\sigma_b(\tau_1) = \sigma(\tau_1), \quad \tau_1 = NF^2, \quad (4.6)$$

for minimal $t = 1$ on the dynamical time scale of the diffusion. It then follows from Eq. (4.5) that

$$A\tau_1 = 5.2,$$

which is used in Figs. 4 and 5. The condition assumed is, of course, somewhat arbitrary but the dependence on A remains extremely weak provided $\tau_1 \ll 1$.

The histogram in Fig. 5 is given in the absolute numbers of trajectory entries into bins in order to graphically demonstrate a negligible number of exceptional crossings of the border. The exact formulation of the Khinchin theorem admits a finite number of crossings in infinite time. Actually, all those “exceptions” are concentrated within a relatively short initial time interval $\tau \sim 1$ (for the accepted A value, see Fig. 4).

The distribution of entropy fluctuations between the borders is characterized by its own big fluctuations due to a large time interval ($\sim \tau$) required for crossing the distribution region (see Eq. (4.3)). The spectacular precipice of many orders of magnitude is reminiscent of a diffusion “shock wave” cutting away the Gaussian tail. The unbounded Gauss curve is also shown in Fig. 5 by the smooth dashed line.

In terms of the variable $S_{\sigma_b} = S_\sigma/R_\sigma$, the standard Gauss law is no longer a stationary distribution (cf. Eq. (3.5)),

$$\sqrt{2\pi}G(S_{\sigma_b}) = R_\sigma(\tau) \exp\left(-\frac{S_{\sigma_b}^2}{2}R_\sigma^2(\tau)\right). \quad (4.7)$$

Both the probability density at the border $|S_{\sigma_b}| = 1$ and the integral probability beyond that are slowly decreasing $\propto 1/\ln(A\tau)$. The “shock wave” decays but still continues to “hold back” the trajectories.

Thus, unlike unrestricted entropy fluctuations out of the equilibrium steady state (Section 1), the strictly restricted fluctuations in the nonequilibrium steady state are well separated, in a short time, from the negative-entropy region, separated in a large excess, that grows in time. In other words, the Poincaré recurrences to any negative entropy quickly and completely disappear leaving the system with ever increasing, even if nonmonotonically, entropy.

As the nonequilibrium steady state involves a heat bath of the infinite phase-space volume (or its nice substitute, the Gauss heat bath), the Poincaré recurrence theorem is not applicable. However, the “anti-recurrence” theorem is not generally true either. For example, the entropy repeatedly crosses the line $S = \tau$ of the average growth in spite of the infinite heat bath, yet it does not do so for the line $S = 0$ of the initial entropy.

We note that the new ratio $\sigma_b^2 \langle S(t) \rangle$ (cf. Eq. (3.4)) represents another “Fluctuation Theorem” as compared to the known one mentioned in Section 3.

5. BIG ENTROPY FLUCTUATIONS IN CRITICAL DYNAMICS

The strict restriction of the global entropy fluctuations in a nonequilibrium steady state considered in the previous section is a result of the “normal,” Gaussian, diffusion of the entropy with a constant rate (4.3) and with the surprising impenetrable border (4.5). In turn, this is related to a particular underlying dynamics of model (1.1) with very strong statistical properties. We note that the border (4.5) has a statistical nature because it is much less than the maximum dynamical fluctuation (3.7).

However, it is well known by now that the homogeneous diffusion can in general be “abnormal” in the sense that the diffusion rate depends on time,

$$D(t) \propto t^{c_D}, \quad -1 \leq c_D \leq 1, \quad (5.1)$$

where c_D is the so-called critical diffusion exponent. The term “critical” refers to a particular class of such systems with a very intricate and specific structure of the phase space (see, e.g., [29] and references therein). The “normal” diffusion corresponds to $c_D = 0$, while a positive $c_D > 0$ represents a superfast diffusion with the upper bound $c_D = +1$, the maximum diffusion rate possible for a homogeneous diffusion. The latter is, of course, the most interesting case for the problem under consideration here. A superslow diffusion for a negative $c_D < 0$ is also possible with the limit $c_D = -1$, which means the absence of any diffusion for $c_D < -1$. An interesting example of a superslow diffusion with $c_D = -1/2$ was considered in [30]. Besides a particular application to the plasma confinement in magnetic field, the example is of a special interest because this slow diffusion is the result of the time-reversible diffusion of particles in a chaotic magnetic field. For other examples and various discussions of abnormal diffusion, see [31].

A number of dynamical models exhibiting the superfast diffusion are known including the limiting case $c_D = 1$ [29, 32]. Interestingly, a simple simulation of the abnormal diffusion is possible by a minor modification of the model under consideration. It concerns the additional 1D map (2.6) only, which now becomes

$$\bar{S} = S + (2p_1 F + F^2)t_s, \quad (5.2)$$

where the new variable t_s is defined by a simple relation

$$t_s = s^{-c_s}, \quad s = 1 - 2|p_1|, \quad (5.3)$$

with s being the distance from any of the two borders $p_1 = \pm 0.5$ homogeneously distributed within the interval ($0 < s < 1$). The quantity $t_s > 1$ describes the sticking of a trajectory in the “critical structure” concentrated

near $s = 0$. Actually, the model does not involve this structure, however its effect is simulated by the “sticking time” t_s that enhances both the fluctuations and the average entropy (5.2). In a sense, this simulation is similar in spirit to that of the Gauss heat bath. All the properties of that sticking are described by a single parameter c_s , the critical sticking exponent ($0 \leq c_s \leq 1$). In particular, it is directly related to the diffusion exponent c_D (see below).

The statistical properties of the abnormal diffusion in this model are determined by the first two moments of the t_s distribution, which can be directly evaluated from the above relations as follows. For the first moment, we have

$$\langle t_s \rangle = \int_0^1 t_s(s) ds = \frac{1}{1-c_s}, \quad c_s < 1, \quad (5.4a)$$

and

$$\langle t_s \rangle \approx \ln \frac{1}{s_1} \approx \ln t, \quad c_s = 1. \quad (5.4b)$$

In the latter case the integral diverges and is determined by the minimum $s \approx s_1 \sim 1/t$ reached over time t that is the total motion time in the iterations of the map. It must be distinguished from the “physical time” in a true model of the critical structure,

$$\tilde{t} \approx t \langle t_s \rangle \approx \begin{cases} \frac{t}{1-c_s}, & c_s < 1, \\ t \ln t, & c_s = 1. \end{cases} \quad (5.5)$$

Similarly, the second moment is given by three relations:

$$\langle t_s^2 \rangle = \frac{1}{1-2c_s}, \quad c_s < \frac{1}{2}, \quad (5.6a)$$

for the normal diffusion,

$$\langle t_s^2 \rangle \approx \ln \frac{1}{s_1} \approx \ln t, \quad c_s = \frac{1}{2}, \quad (5.6b)$$

in the critical case, and

$$\langle t_s^2 \rangle \approx \frac{s_1^{1-2c_s}}{2c_s-1} \approx \frac{t^{2c_s-1}}{2c_s-1}, \quad \frac{1}{2} < c_s \leq 1, \quad (5.6c)$$

for the superfast diffusion.

The average entropy production is found from Eq. (5.2) as

$$\langle S(t) \rangle = NF^2 t \langle t_s \rangle = NF^2 \tilde{t} \equiv \tau, \quad (5.7)$$

with the redefined time variable τ (cf. Eq. (3.3)). In this section, we only consider the simplest case of a single trajectory ($N = 1$).

Evaluating the superfast diffusion requires a slightly different averaging $\langle (2p_1 t_s)^2 \rangle$ (see Eq. (5.2)). However,

it is easily verified that asymptotically as $\tau \rightarrow \infty$, the difference with respect to Eq. (5.6c) vanishes, and one arrives at the following estimate for the critical rms dispersion σ_{cr} :

$$\frac{\sigma_{cr}^2(\tau)}{B^2} = \tilde{t}D(\tilde{t}) = F^2 \langle t_s^2 \rangle t = \frac{(1-s_s)^{2c_s} \tau^{2c_s}}{2c_s - 1 F^{4c_s - 2}} \quad (5.8a)$$

if $1/2 < c_s < 1$ (5.6c), and

$$\frac{\sigma_{cr}(\tau)}{B} = \frac{\tau}{F \ln(\tau/F^2)} \quad (5.8b)$$

in the most interesting limiting case where $c_s = 1$. The empirical factor $B \sim 1$ accounts for all the approximations in the above relations.

The limit as $c_s \rightarrow 1$ in Eq. (5.8a) crucially differs from the limiting relation (5.8b). The origin of this discrepancy is Eq. (5.4a). A more accurate evaluation for $c_s \approx 1$ reads

$$\begin{aligned} \langle t_s \rangle &= \int_{s_1}^1 t_s(s) ds \\ &= \frac{1 - s_1^{1-c_s}}{1 - c_s} = \frac{1 - \exp[(1 - c_s) \ln s_1]}{1 - c_s}, \end{aligned} \quad (5.9)$$

where $s_1 \sim 1$ is the minimum s over t iterations of the map (cf. Eq. (5.4b)). Relation (5.4a) is therefore valid under the condition $\epsilon \ln t > 1$ only (with $\epsilon = 1 - c_s$), while in the opposite limit, we have $\langle t_s \rangle \approx \ln t$ as for $c_s = 1$, Eq. (5.4b). The crossover between the two scalings occurs at

$$t_{cro} \sim e^{1/\epsilon}, \quad \tau_{cro} \sim \frac{e^{1/\epsilon}}{\epsilon} F^2. \quad (5.10)$$

The deviation from Eq. (5.8a) is essential for a sufficiently small ϵ only.

The ratio of fluctuations to the average entropy production is given by the reduced entropy (see Eq. (4.4))

$$S_g = \pm \frac{\sigma_{cr}}{\tau} \approx \frac{B}{F \ln(\tau/F^2)}, \quad (5.11)$$

where the latter expression is estimate (5.8b) for the rms fluctuations. They are slowly decreasing with time, and at

$$\tau \approx \tau_0 = F^2 \exp(1/F),$$

the rms line crosses the border $S_g = -1$ of zero entropy. Afterwards, the entropy remains mainly positive. To be more precise, the probability for a trajectory to enter into the negative-entropy region is systematically decreasing with time, although rather slowly. This must be compared with the F -independent crossover $\tau_0 = 1/3$ and a rapid drop of the probability to return to $S < 0$ for the normal diffusion (Section 4).

However, there exists another mechanism of big fluctuations, specific for the critical dynamics. Namely, a separated individual fluctuation can be produced as the result of a single extremely big sticking time t_s over the total motion up to the moment the fluctuation springs up in a single map iteration. We recall that in the present model, each sticking corresponds to just one map iteration. The increments of dynamical variables in this jump are obtained from Eq. (5.2) as

$$\Delta S = \pm F t_s, \quad \Delta \tau = F^2 t_s, \quad (5.12)$$

where $t_s \gg 1$ (with $2p_1 \approx 1$) is assumed (a big fluctuation). The reduced fluctuation is then given by

$$S_g \approx \frac{S}{\tau} = \pm \frac{F t_s}{\tau + F^2 t_s} \approx \pm \frac{1/F}{1 + \tau/\Delta \tau}. \quad (5.13)$$

The maximum single sticking time over the motion time t is, on the average,

$$\langle t_s \rangle \approx t \ln t = \frac{\tau}{F^2}. \quad (5.14)$$

Therefore, a single fluctuation (5.13) has the upper bound

$$|S_g| \leq \frac{A}{F}, \quad (5.15)$$

where an empirical factor $A \sim 1$ is introduced similarly to Eq. (5.8b).

The border (5.15) considerably exceeds the rms diffusion fluctuation (5.11) and, even more importantly, the former never crosses the zero-entropy line $S_g = -1$. Therefore, the critical fluctuations repeatedly bring the system into the negative-entropy region. This is because the upper bound (5.15) does not depend on time τ provided that $\Delta \tau \geq \tau$ in Eq. (5.13). However, in a chain of successive fluctuations, the values of τ in Eqs. (5.13) and (5.14) are not generally equal. While in the former relation it is always the total motion time as assumed above, it must be the preceding period of fluctuations in Eq. (5.14): $\tau_n \rightarrow P_n < \tau_n$, where n is the serial number of fluctuations. Hence, the approach to the upper bound (5.15) is only possible under the condition $P_n \geq P_{n-1}$, which implies $P_n \approx \tau_n$. Thus, the fluctuations become more and more rare with the period growing exponentially in time. In other words, the fluctuations are stationary in $\ln \tau$ with a sufficiently big mean period $\langle \ln P \rangle \approx 5$ (see Fig. 6).

In Fig. 6, an example of several big critical fluctuations in the limiting case $c_s = 1$ is presented for five single sufficiently long trajectories with different initial conditions and the motion time up to $\tau \approx 5 \times 10^9$ and $t = 10^{10}$ iterations. To achieve such a long time, the force was increased up to $F = 0.1$ (see Eq. (5.14)).

Unlike a similar Fig. 4 for the normal diffusion, only several big fluctuations with $F|S_g| > 0.3$ are presented in Fig. 6. For the full picture of critical fluctuations, the

required output becomes formidably long. The distribution of all fluctuations, independent of time, is shown in Fig. 7.

Each fluctuation in Fig. 6 is presented by a pair of FS_g values connected by the straight line: one at a map iteration just before the fluctuation (circles), and the other (stars) at the next iteration when the fluctuation springs up (see above). Both are plotted at the same, latter, τ to follow the pairs. This slightly shifts the circles to the right.

The most important, if only preliminary, result of numerical experiments is the confirmation of the fluctuation upper bound (5.15) that is independent of time. As expected, the circles represent considerably smaller $F|S_g|$ values, roughly following the diffusive scaling (5.11).

The border (5.15) qualitatively reminds the strict upper bound for the normal diffusion (Section 4), including a logarithmic ratio with respect to the rms size (4.5), as compared to the ratio

$$R_{cr}(\tau) \approx \ln(\tau/F^2) \quad (5.16)$$

in the critical diffusion. An interesting question whether the new, critical, border is also as strict as the old one in the normal diffusion remains, to my knowledge, open, at least for the physical model under consideration where the superdiffusion is caused by a strong long-term correlation of successive entropy changes due to the sticking of trajectory.

However, for a much simpler problem of statistically independent changes, various generalizations of Khinchin theorem to the abnormal diffusion were proved by many mathematicians (see, e.g., [33]). In the present model, this is precisely the case for description in the map time t with statistically independent iterations. The most general and complete result was recently obtained by Borovkov [34]. In the present notation, it can be approximately represented in a very simple form for the ratio

$$R_{cr} = \frac{\sigma_b}{\sigma} \sim (\ln t)^{c_s} \quad (5.17)$$

in the entire superdiffusion interval ($1/2 < c_s \leq 1$). For the most important reduced fluctuation (5.13), we then arrive at the two relations

$$|S_g| \approx \frac{\sigma_b}{\tau} \sim \frac{\tau^{c_s-1}}{F^{2c_s-1}} \left(\ln \frac{\tau}{F^2} \right)^{c_s} \quad (5.18a)$$

for $c_s < 1$ and

$$|S_g| \approx \frac{\sigma_b}{\tau} \sim \frac{1}{F} \quad (5.18b)$$

in the limiting case $c_s = 1$. The latter confirms estimate (5.15), which, in turn, is in a good agreement with the empirical data in Fig. 6. In any event, a simple phys-

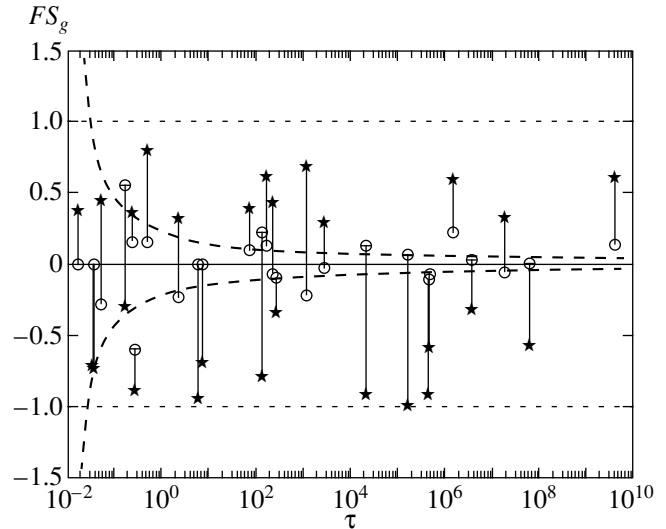


Fig. 6. Time dependence of 26 big fluctuations in critical dynamics: 5 single trajectories up to 10^{10} iterations, $c_s = 1$, $F = 0.1$. Only fluctuations with $F|S_g| > 0.3$ are shown, each by a pair of points connected by the straight line: the big fluctuation itself (stars) and at the preceding map iteration (circles, see text). Two dashed curves show the rms fluctuations of $F|S_g|$, Eq. (5.11), with $B = 1$. Horizontal dotted lines mark the upper bound, Eq. (5.15), with $A = 1$.

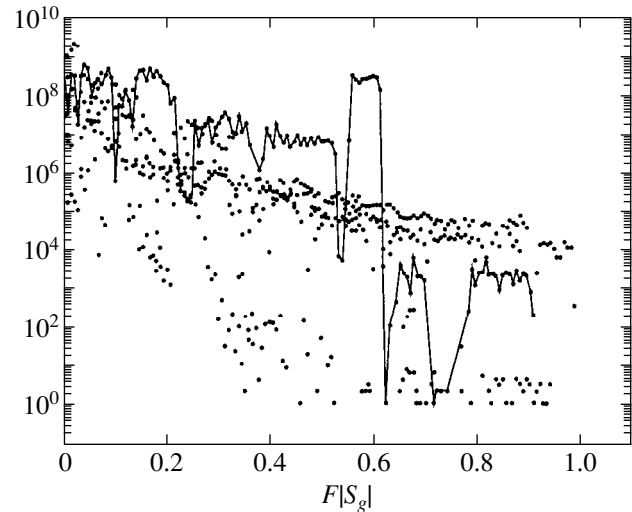


Fig. 7. Histogram of critical fluctuations in the number of entries per bin of width 0.007 for the data in Fig. 6. The border $S = 0$ corresponds to $F|S_g| = -F = -0.1$. The points for the longest trajectory are connected by line.

ical estimate (5.15) seems to provide an efficient description of the fluctuation upper bound.

In Fig. 7, an example of all (at each map's iteration) fluctuations is shown for the data from the same runs as in Fig. 6. In addition to very large overall distribution fluctuations, a sharp drop by about four orders of magnitude is clearly seen near the expected upper

bound (5.15). It is similar to the drop in Fig. 5 for the normal diffusion.

Thus, the critical diffusion results in infinitely many recurrences far into the negative-entropy region $S < 0$ (for $F \ll 1$), the sojourn time in that region being comparable to the total motion time. Of course, the former is less than 50% on the average, so that asymptotically in time the entropy is always growing. In this respect, the global critical fluctuations are similar to the local ones in the normal diffusion (Section 3).

We note, however, that the upper bound $\sigma_b/\tau \sim 1/F$ (5.18b) is permanent in the strict limit $c_s = 1$ only. For any deviation from the limit $\epsilon = 1 - c_s > 0$, this bound lasts a finite time determined by the crossover (5.10) ($\tau \lesssim F^2 \exp(1/\epsilon)/\epsilon$) to decreasing $\sigma_b/\tau \rightarrow 0$, Eq. (5.18a). Another interesting representation of this intermediate behavior is the crossover in the sticking exponent,

$$\epsilon \lesssim \frac{1}{\ln(\tau/F^2)} \approx F|S_g|, \quad (5.19)$$

which is actually shown in Fig. 6 by the upper dashed line. For the longest $\tau = 5 \times 10^9$, the latter crossover is $\epsilon_{cro} \approx 0.037$.

Again, the new cardinally different critical ratio $\sigma_b^2/\langle S(t) \rangle$ and the distribution of entropy fluctuations lead to yet another ‘‘Fluctuation Theorem’’ as compared to the two previous ones mentioned in Sections 3 and 4.

6. DISCUSSION AND CONCLUSIONS

In the present paper, the results of extensive numerical experiments on big entropy fluctuations in a non-equilibrium steady state of classical dynamical systems are presented and their peculiarities are analyzed and discussed. For comparison, some similar results for the equilibrium steady state are briefly described in the Introduction (they will be published in detail elsewhere [10]).

All numerical experiments have been carried out on the basis of a very simple model, the Arnold cat map (1.1) on a unit torus, with only three minor, but important, modifications that allowed comprising all the problems under consideration. The modifications are:

(1) The expansion of the torus in the p direction (1.2), which allows more impressive diffusive fluctuations out of the equilibrium steady state (Fig. 1 in Section 1).

(2) The addition of 1D map (2.5) with the constant driving force F and with an ingenious time-reversible friction force that represents the so-called Gauss heat bath and which allows modeling a physical thermostat of infinitely many degrees of freedom [20, 21]. This is the principal modification in the present studies of fluctuations in a nonequilibrium steady state (Sections 3–5).

(3) The addition of a new parameter t_s , Eq. (5.3), in map (5.2) which allows for the study of very unusual fluctuations of an ‘‘abnormal,’’ critical, dynamical diffusion (Section 5).

Big fluctuations in the equilibrium steady state are briefly considered in Section 1. The simplest one of this class, which we call the Boltzmann fluctuation, is shown in Fig. 1. It is obviously symmetric under time reversal, and at least in this case, therefore, there is no physical reason for the notorious ‘‘time arrow’’ concept. Nevertheless, a related concept, for example, the thermodynamic arrow, pointing in the direction of the average increase of entropy, makes sense in spite of the time symmetry. The point is that the relaxation time of the fluctuation is determined by the model parameter C only, and does not depend on the fluctuation itself. On the contrary, the expectation time for a given fluctuation, or the mean period between successive fluctuations, rapidly grows with the fluctuation size and with the number of trajectories (or degrees of freedom).

Besides the simplest Boltzmann fluctuation, various others are also possible, typically with a much smaller probability. One of those—the two correlated Boltzmann fluctuations, which we call the Schulman fluctuation—was recently described in [36] using the same Arnold cat map. However, this model is not related to cosmology as was speculated in [36]. At least, the Universe and most of the macroscopic phenomena therein require qualitatively different models, ones without an equilibrium steady state. These structures do appear (with a probability of 1) as a result of certain regular collective processes that lead to very complicated non-equilibrium and inhomogeneous states with ever increasing entropy. This is in contrast with a constant, on the average, entropy in ES systems.

A nonequilibrium steady state, the main subject of this paper, is but a little, characteristic though, piece of the chaotic collective processes. In model (2.5), the driving force F represents a result of some preceding collective processes, the spring of free energy, and the Gauss friction does so for an infinite environment around, the sink of the energy, converting the work into heat, on the average. An interesting peculiarity of these systems is that the big fluctuations can, and under certain conditions, do the opposite, converting some heat back into the work.

Two types of fluctuations were studied:

(i) the local ones on a set of trajectory segments of length- t_1 iterations and of the entropy change S_i (Section 3), and

(ii) ones of the global entropy $S(t)$ along a trajectory with respect to the initial entropy set to zero, $S(0) = 0$ (Sections 4 and 5).

The former were found to have a stationary unrestricted distribution close to the standard Gauss law with some enhancement of an unknown mechanism for large fluctuations. The study of the latter effect will be continued. The distribution is symmetric with respect

to the average entropy, growing in proportion to time in agreement with previous studies on a more complicated (and more realistic) model [27]. Even though the distribution is asymmetric with respect to zero entropy change, the probability of negative $S_i < 0$ is generally not small provided $F^2 N t_1 \lesssim 1$. This phenomenon, apparently a new one in the nonequilibrium steady state, was first observed in [27] but has been interpreted there as a violation of the Second Law. It seems to be the reflection of a common, but wrong in my opinion, understanding of the Second Law as a monotonic growth of entropy, neglecting all the fluctuations including the large ones. The nonmonotonic rise of entropy is clearly seen, for instance, in Fig. 4, and discussed in detail in Sections 3 and 4.

The behavior of global entropy is completely different as the data in the same Fig. 4 demonstrate (Section 4). Although the entropy evolution remains non-monotonic, it quickly crosses the line of the initial zero entropy and does not return into the negative entropy region $S < 0$. This is insured by the famous Khinchin theorem about the strict upper bound for the diffusion process. At least for physicists, this limitation of a statistical nature for a random motion is surprising and apparently less known. That unidirectional evolution is the most important distinction of the nonequilibrium steady states from the equilibrium ones. In particular, it leads to a certain asymmetry of the entropy distribution sometimes called the “Fluctuation Theorem” or “Fluctuation Law”. However, one should bear in mind that this law essentially depends on the underlying dynamics as briefly discussed in Sections 3–5.

This characteristic feature of nonequilibrium steady state further justifies the concept of the thermodynamic arrow pointing to a larger, on the average, entropy. Yet, again it is not related to the properties of time. Of course, the entropy will systematically decrease upon formal time reversal, which is also the case with the model under consideration because the Gauss heat bath is time reversible. Within the steady state approximation, or rather restriction, this would be an infinitely large fluctuation that never comes to the end. However, this fluctuation would never occur either, as a result of the natural time evolution of the system, opposite to the case of equilibrium fluctuations. The ultimate origin of that crucial difference is that the former process, even asymptotically in time, is a tiny little part of the full underlying dynamics of an infinite system. In particular, the initial state $S(0) = 0$ is not a result of the preceding fluctuation, as is the case in ES, but has been eventually caused, for instance, by instability of the initial ES at a very remote time in the past. If one imagined the time reversal at that instant, nothing would change because the thermodynamic arrow does not depend on the direction of time provided, of course, the time reversible fundamental dynamics. Precisely this universal overall dynamics unifies the time for all the interacting objects like particles and fields throughout the

Universe. In particular, it is incompatible with the two opposite time arrows (an old Boltzmann’s hypothesis [2] that still has some adherents [36]).

Coming back to nonequilibrium steady states, it is worth mentioning that the regularities of the fluctuations in those, both local and global, can be applied, at least qualitatively, to a small part of a big fluctuation in a statistical equilibrium (Fig. 1) on both sides of the maximum. This interesting question will be considered in detail elsewhere [10].

Finally, some preliminary numerical experiments on the global entropy fluctuations and the theoretical analysis were carried out in a special case of the critical dynamics, which turned out to be the most interesting one for the problem in question (Section 5). The point is that the critical dynamics leads to the “abnormal” superdiffusion with the rate $D \propto \tau^{2c_s-1}$ and the rms fluctuation size $\sigma_{cr} \propto \tau^{c_s}$, where c_s is a new parameter of the third model ($1/2 < c_s \leq 1$). This implies that for $c_s \approx 1$, the reduced entropy $|S_g| \propto \tau^{c_s-1}$ decreases very slowly compared to the normal diffusion $|S_g| \propto 1/\sqrt{\tau}$. In the limiting case where $c_s = 1$, the entropy $|S_g| \propto 1/\ln \tau$ is still decreasing. However, in addition to diffusive fluctuations, there is a set of infinitely many separated fluctuations whose size does not decrease with time (Fig. 6). In other words, these preliminary numerical experiments suggest that in the limiting case of the critical dynamics, the Poincaré recurrences to the initial state $S = 0$ and beyond repeatedly occur without limit. These are preliminary results to be confirmed and further studied in detail.

In this paper, we only considered the fluctuations in classical mechanics. In general, the quantum fluctuations must be significantly different. However, according to the Correspondence Principle, the dynamics and statistics of a quantum system in the semiclassical regime must be close to the classical ones on the appropriate, generally finite, time scales (for details, see [12, 35]). Interestingly, the computer classical dynamics (that is, the simulation of a classical dynamical system on digital computer) is of a qualitatively similar character. This is because any quantity is discrete (“overquantized”) in the computer representation. As a result, the correspondence between the classical continuous dynamics and its computer representation in numerical experiments is restricted to certain finite time scales as in quantum mechanics (see the first two references in [35]).

The discreteness of computer phase space leads to another peculiar phenomenon: generally, the computer dynamics is irreversible because of the rounding-off operation unless the special algorithm is used in numerical experiments. Nevertheless, this does not affect the statistical properties of chaotic computer dynamics. In particular, the statistical laws in computer representation remain time-reversible in spite of the (nondissipative) irreversibility of the underlying dynamics. This

simple example demonstrates that contrary to a common belief, the statistical reversibility is a more general property than the dynamical one.

In the very conclusion, we briefly remark on a very difficult, complicated and vague problem, the so-called (physical) causality principle, i.e., the time-ordering of the cause and the effect. A detailed discussion of this important problem will be published elsewhere [37]. We only note the example of a simple Boltzmann fluctuation shown in Fig. 1. I adhere to the idea of statistical nature of causality. Indeed, the cause is, by definition, an “absolutely” independent event that is only possible in the chaotic dynamics. Moreover, the concept of cause loses its usual physical meaning in any purely dynamical description. For example, the initial conditions precisely determine the entire infinite trajectory ($-\infty < t < \infty$), i.e., both the future and the past of such a “cause.” For a single Boltzmann fluctuation, an appropriate cause is the minimum entropy (at $t = t_i$ in Fig. 1). This was exactly the procedure used in numerical experiments for the location of a fluctuation of an approximately given size. The principal difference from the exact dynamical initial conditions is that the former cause is an approximate (e.g., average) fluctuation size, which is sufficient for the complete statistical description of the fluctuation, however it leaves enough freedom for the independence from other events, including the preceding fluctuations. However, this cause determines not only the future relaxation of the fluctuation (in agreement with the causality principle) but also the past rise of the same fluctuation, which is a violation of causality, or acausality (spontaneous rise of a fluctuation), or anti-causality, which is perhaps the most appropriate term. Upon the time reversal, the causality/anticausality exchange, which allows for the concept of the causality arrow, however this is not related to the physical time. In this philosophy, the directions of the thermodynamic and causal arrows, coincide independently of the direction of time. An important point of this philosophy is that the “arrow” concept is related to the interpretation of a physical phenomenon rather than to the phenomenon itself. In particular, the question “how to fix or maintain the arrow” [36] is up to the researcher alone. In a more complicated Schulman’s double fluctuation, the causality mechanism becomes more interesting [36], and will be discussed in [37] from a different point of view.

I am grateful to Wm. Hoover for attracting my attention to a new class of highly efficient dynamical models with the Gauss heat bath and for stimulating discussions and suggestions. I very much appreciate the initial collaboration with O.V. Zhirov. I am also indebted to A.A. Borovkov for elucidation of Khinchin theorem and of its recent generalizations to the “abnormal” superdiffusion.

REFERENCES

1. D. G. Luchinsky, P. McClintock, and M. I. Dykman, Rep. Prog. Phys. **61**, 889 (1998).
2. L. Boltzmann, *Vorlesungen über Gastheorie* (J. A. Barth, Leipzig, 1896–98); *Lectures on Gas Theory* (Univ. of California Press, Berkeley, 1964; Gostekhizdat, Moscow, 1956).
3. E. Schrödinger, *Über die Umkehrung der Naturgesetze* (Sitzungsber. Preuss. Akad. Wiss., 1931), p. 144.
4. A. N. Kolmogoroff, Math. Ann. **113**, 766 (1937); **112**, 155 (1936); *Selected Papers on Probability Theory and Mathematical Statistics*, Ed. by Yu. V. Prokhorov (Nauka, Moscow, 1986), p. 197, p. 173.
5. A. M. Yaglom, Dokl. Akad. Nauk SSSR **56**, 347 (1947); Mat. Sb. **24**, 457 (1949).
6. *Proceedings of the 20th IUPAP International Conference on Statistical Physics, Paris, 1998*, Physica A (Amsterdam) **263**, 516 (1999).
7. I. P. Kornfeld, S. V. Fomin, and Ya. G. Sinai, *Ergodic Theory* (Nauka, Moscow, 1980; Springer-Verlag, New York, 1982).
8. V. I. Arnold and A. Avez, *Ergodic Problems of Classical Mechanics* (Benjamin, New York, 1968; RCD, Izhevsk, 1999).
9. A. Lichtenberg and M. Leiberman, *Regular and Chaotic Dynamics* (Springer-Verlag, New York, 1992); *Regular and Stochastic Motion* (Springer-Verlag, New York, 1982; Mir, Moscow, 1984).
10. B. V. Chirikov and O. V. Zhirov, E-print archives nlin-CD/0010056.
11. D. V. Anosov, Dokl. Akad. Nauk SSSR **145**, 707 (1962).
12. B. V. Chirikov, in *Law and Prediction in the Light of Chaos Research*, Ed. by P. Weingartner and G. Schurz (Springer-Verlag, Berlin, 1996), p. 10; Open Syst. Inf. Dyn. **4**, 241 (1997); E-print archives chao-dyn/9705003.
13. L. D. Landau and E. M. Lifshitz, *Statistical Physics* (Nauka, Moscow, 1995; Pergamon, Oxford, 1980), Part I.
14. B. V. Chirikov, Wiss. Z. Humboldt Univ. Berlin, Ges.-Sprachwiss. Reihe **24**, 215 (1975).
15. J. Jeans, Philos. Trans. R. Soc. London, Ser. A **199**, 1 (1929).
16. H. Haken, *Synergetics* (Springer-Verlag, Berlin, 1978; Mir, Moscow, 1980).
17. A. Turing, Philos. Trans. R. Soc. London, Ser. B **237**, 37 (1952); G. Nicolis and I. Prigogine, *Self-Organization in Nonequilibrium Systems* (Wiley, New York, 1977).
18. A. Cottrell, in *The Encyclopedia of Ignorance*, Ed. by R. Duncan and M. Weston-Smith (Pergamon, New York, 1977), p. 129.
19. P. Glansdorf and I. Prigogine, *Thermodynamic Theory of Structure, Stability, and Fluctuations* (Wiley, New York, 1971; Mir, Moscow, 1972).
20. D. Evans and G. Morriss, *Statistical Mechanics of Nonequilibrium Liquids* (Academic, New York, 1990); Wm. G. Hoover, *Computational Statistical Mechanics* (Elsevier, New York, 1991); in *Proceedings of the Workshop on Time-Reversal Symmetry in Dynamical Systems, Warwick, 1996*; Physica D (Amsterdam) **112** (1–2), 225 (1998).

21. Wm. Hoover, *Time Reversibility, Computer Simulation, and Chaos* (World Scientific, Singapore, 1999).
22. N. I. Chernov, G. Eyink, J. Lebowitz, and Ya. G. Sinai, *Phys. Rev. Lett.* **70**, 2209 (1993).
23. R. Peierls, in *Theoretical Physics in Twentieth Century*, Ed. by M. Fierz and V. Weisskopf (Wiley, New York, 1961).
24. K. Gauss, *J. Reine Angew. Math.* **4**, 232 (1829).
25. Wm. Hoover, *Phys. Lett. A* **255**, 37 (1999).
26. F. Galton, *Natural Inheritance* (Macmillan, London, 1889).
27. D. Evans, E. Cohen, and G. Morriss, *Phys. Rev. Lett.* **71**, 2401 (1993).
28. A. Ya. Khinchin, *C. R. Hebd. Seances Acad. Sci.* **178**, 617 (1924); in *Selected Papers on Probability Theory*, Ed. by B. V. Gnedenko and A. M. Zubkov (TVP, Moscow, 1995), p. 10.; M. Loève, *Probability Theory* (Van Nostrand, Princeton, 1955); A. A. Borovkov, *Probability Theory* (Nauka, Moscow, 1986).
29. B. V. Chirikov and D. L. Shepelyansky, *Physica D (Amsterdam)* **13**, 395 (1984); B. V. Chirikov, *Chaos, Solitons and Fractals* **1**, 79 (1991).
30. A. Rechester and M. Rosenbluth, *Phys. Rev. Lett.* **40**, 38 (1978); B. V. Chirikov, *Open Syst. Inf. Dyn.* **4**, 241 (1997); E-print archives chao-dyn/9705003.
31. P. Levy, *Théorie de l'Addition des Variables Eléatoires* (Gauthier-Villiers, Paris, 1937); T. Geisel, J. Nierwetberg, and A. Zacherl, *Phys. Rev. Lett.* **54**, 616 (1985); R. Pasmantier, *Fluid Dyn. Res.* **3**, 320 (1985); Y. Ichikawa *et al.*, *Physica D (Amsterdam)* **29**, 247 (1987); R. Voss, *Physica D (Amsterdam)* **38**, 362 (1989); G. M. Zaslavskii, M. Yu. Zakharov, A. I. Neishtadt, *et al.*, *Zh. Éksp. Teor. Fiz.* **96**, 1563 (1989) [*Sov. Phys. JETP* **69**, 885 (1989)]; H. Mori *et al.*, *Prog. Theor. Phys. Suppl.*, No. 99, 1 (1989).
32. B. V. Chirikov, *Zh. Éksp. Teor. Fiz.* **110**, 1174 (1996) [*JETP* **83**, 646 (1996)]; B. V. Chirikov and D. L. Shepelyansky, *Phys. Rev. Lett.* **82**, 528 (1999).
33. J. Chover, *Proc. Am. Math. Soc.* **17**, 441 (1966); T. Mikosh, *Vestn. Leningrad. Univ.*, No. 13, 35 (1984); Yu. S. Khokhlov, *Vestn. Mosk. Univ.*, No. 3, 62 (1995).
34. A. A. Borovkov, submitted to *Sib. Mat. Zh.* (2000).
35. B. V. Chirikov, F. M. Izrailev, and D. L. Shepelyansky, *Sov. Sci. Rev., Sect. C* **2**, 209 (1981); B. V. Chirikov, in *Lectures in Les Houches Summer School on Chaos and Quantum Physics, 1989* (Elsevier, Amsterdam, 1991), p. 443; G. Casati and B. V. Chirikov, in *Quantum Chaos: Between Order and Disorder*, Ed. by G. Casati and B. V. Chirikov (Cambridge Univ. Press, Cambridge, 1995), p. 3; *Physica D (Amsterdam)* **86**, 220 (1995); B. V. Chirikov, in *Proceedings of the International Conference on Nonlinear Dynamics, Chaotic and Complex Systems, Zakopane, 1995*, Ed. by E. Infeld, R. Zelazny, and A. Galkowski (Cambridge Univ. Press, Cambridge, 1997), p. 149; B. V. Chirikov and F. Vivaldi, *Physica D (Amsterdam)* **129**, 223 (1999).
36. L. S. Schulman, *Phys. Rev. Lett.* **83**, 5419 (1999); G. Casati, B. V. Chirikov, and O. V. Zhirov, *Phys. Rev. Lett.* **85**, 896 (2000); L. S. Schulman, *Phys. Rev. Lett.* **85**, 897 (2000).
37. B. V. Chirikov, private communication (2000).